J. Fluid Mech. (1978), *vol.* 87, *part* 1, *pp.* 143–158
Printed in Great Britain

A harbour theory for wind-generated waves based on ray methods

By JESPER LARSEN

Laboratory of Applied Mathematical Physics, Technical University of Denmark, Copenhagen†

(Received 8 September 1977)

In the paper we consider harbour oscillations excited by wind-generated gravity waves. The analysis is based on the fact that waves propagate along rays (wave orthogonals). In this way the elliptic boundary-value problem is turned into an initial-value problem along each ray. When a ray strikes the boundary (the harbour walls), reflected rays are produced in accordance with the law of reflexion. When a ray strikes an edge point of the boundary (e.g. the tip of a breakwater) diffracted rays are produced and emitted in all directions into the harbour. Algorithms for the tracing of incident, multiply reflected and singly diffracted rays as well as the computation of the field on each ray are presented. Attenuation mechanisms (e.g. partial reflexion), which limit the number of rays needed to compute the field, are included. Numerical examples for a rectangular and an actual harbour are given. A comparison between the results obtained by ray methods and finite difference methods is included.

1. Introduction

Analytic and numerical treatment of the diffraction of water waves was originated by Sommerfeld (1896) through his solution to the 'half-plane problem'. Penney & Price (1944) used the solution to construct the diffracted field behind a semi-infinite breakwater. Blue & Johnson (1949) used an approximate solution for the breakwater gap for the construction of amplitude diagrams. Separate diagrams for different ratios of gap width to wavelength are required. The reflexion of waves inside the harbour was not included in their model. Carr (1952) showed a graphical way of treating also the reflexion of waves inside the harbour using the law of reflexion. The method was limited to harbours with only a few straight harbour sides and a narrow harbour entrance. For a survey of these graphical methods see Ippen (1966).

Resonant harbour oscillations were treated analytically by Miles & Munk (1961) through their formulation of the 'harbour paradox'. Ippen & Goda (1963) investigated theoretically the problem of long wave excited resonance in a rectangular harbour. In the early seventies a number of numerical models for the calculation of harbour oscillations were put forward. Hwang & Tuck (1970) and Lee (1971) used integral equation methods. Berkhoff (1973) and Mei & Chen (1975) based their models on finite element methods. In contrast to integral equation methods the finite element methods yield solutions for variable depth. Recently a nonlinear model for shallow-water waves in harbours based on finite difference methods has been developed by

† Present address: The Institute of Mathematical Technology, Sommervej 7, DK 2920 Charlottenlund, Denmark.

the Danish Hydraulic Institute (private communication). Common to all these models is the discretization of the harbour area or harbour boundary. Some of the models have been used for the computation of harbour oscillations excited by shorter waves; but, owing to the discretization of the harbour area, the computational effort grows strongly with the wavenumber.

For wind-generated waves the wavelength is usually short compared with the horizontal dimensions in the harbour, and asymptotic methods should be used. The ray method is an asymptotic method in the relative wavenumber; the approximation becomes better and better as the wavelength tends to zero. An account of the modern ray method may be found in Keller (1962). In Keller (1958) the theory is applied to surface waves on water. Shen, Meyer & Keller (1968) treat waves in channels and around islands. For a survey of the general asymptotic method see Shen (1975). Christiansen (1975, 1976) uses ray methods for the construction of solutions to specific problems.

The ray method is based on the fact that waves propagate along rays (wave orthogonals). This is stated mathematically by assuming an asymptotic representation for the wave field explicitly using the fact that the wavelength relative to the horizontal dimensions in the problem is small (actually the wavelength needs only to be smaller than the horizontal dimensions). Insertion of the assumption in the governing elliptic differential equation yields differential equations for the determination of the rays – the eikonal equation – and the determination of the field on the rays – the transport equation. In this way the elliptic boundary-value problem is turned into an initial-value problem along each ray.

When a ray strikes the surface of a scatterer (e.g. a wall in the harbour) a reflected ray is produced in accordance with the law of reflexion. The field on the reflected ray is determined from the field on the incident ray by multiplication with a reflexion coefficient. The reflexion coefficient must be determined from a canonical problem, i.e. the simplest problem that contains all pertinent features of the process in question. When a ray strikes an edge point in the harbour (e.g. the tip of a breakwater) diffracted rays are produced and emitted in all directions into the harbour in accordance with the law of edge diffraction (Keller 1962). Again, the field on the diffracted ray is described by a diffraction coefficient determined from a canonical problem. Attenuation mechanisms due to partial reflexion, bottom friction, and the divergence of diffracted rays are included in the theory.

In the present work we describe an algorithm developed for the determination of incident, multiply reflected and singly diffracted rays. Since, in the present paper, the water depth is assumed to be constant the rays are straight. The theory is also valid for variable water depth, in which case the tracing of refracted rays must be included in the above-mentioned algorithm. This extension has been carried out and will be described in a future paper. When the field on each ray is determined the various attenuation mechanisms mentioned above are taken into account. The attenuation due to bottom friction and divergence of diffracted rays is obtained by solution of the transport equation. Partial reflexion is described by a linear surface impedance boundary condition. This boundary condition forms the basis for the canonical problems determining the reflexion and diffraction coefficients.

According to the reciprocity principle the propagation direction along the rays can be inverted. This fact is used in the procedure for the ray-tracing algorithm. A source

is placed at the point in the harbour where we want to determine the wave field and this source radiates rays in all directions. The algorithm then singles out the rays which – directly, after single or multiple reflexions or single diffractions – can be identified with an inverted incident ray. The incident field is taken to be a plane sinusoidal wave train. Numerical results are shown for a rectangular harbour and an actual harbour.

2. The analysis

A definition sketch for the problem is shown in figure 1. For the surface elevation $H(x, y, t)$ we assume time harmonic variation, i.e.

$$H(x, y, t) = Re\,[\eta(x, y) \exp(-i\omega t)]. \tag{1}$$

Here x and y are horizontal co-ordinates (figure 1), ω is the angular frequency $2\pi/T$ (T is the wave period) and i is the imaginary unit. Assuming irrotational flow in an incompressible fluid and a weakly varying bed, a linear equation for the spatial part $\eta(x, y)$ of the surface elevation can be deduced (see Smith & Sprinks 1975):

$$\nabla . (p \nabla \eta) + k^2 p \eta = 0. \tag{2}$$

This equation – the mild-slope equation – is correct to the first order in the bottom slope. In (2) ∇ is the horizontal gradient operator and p is given by

$$p = gh \frac{\tanh kh}{kh} \frac{1}{2} \left(1 + \frac{2kh}{\sinh 2kh}\right), \tag{3}$$

in which k is the local wavenumber $2\pi/L$ (L is the local wavelength) related to ω and the water depth h through the dispersion relation

$$\omega^2 = gk \tanh kh, \tag{4}$$

where g is the acceleration due to gravity. In two cases (2) reduces to the Helmholtz equation, viz. for deep water ($kh \to \infty$) or constant water depth. In both cases we have

$$(\nabla^2 + k^2)\,\eta = 0, \tag{5}$$

which is used in the present paper. The attenuation due to bottom friction can be described linearly by replacing k by the complex constant $k_1 = k + i\alpha$ in (5) (see Larsen 1977*a*). Here α is given by

$$\alpha = \frac{1}{\pi} \frac{2kh}{2kh + \sinh 2kh} \frac{k_N}{h} k, \tag{6}$$

where k_N is a friction parameter of dimension length (Jonsson 1975).

In this paper we use the most general linear boundary condition for the surface elevation, i.e. the surface impedance boundary condition with surface impedance Z,

$$\frac{\partial \eta}{\partial n} + ikZ\eta = 0, \quad \text{at the boundary,} \tag{7}$$

at the vertical plane boundary, with n normal to this plane and pointing into the harbour area (figure 1). The harbour is connected to the open sea and we need the radiation condition

$$\lim_{r \to \infty} r^{\frac{1}{2}} \left(\frac{\partial \eta^S}{\partial r} - ik\eta^S\right) = 0 \tag{8}$$

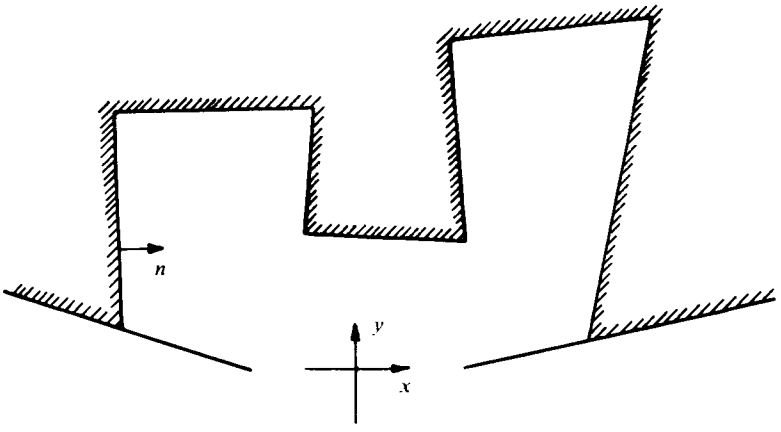

FIGURE 1. Definition sketch.

to ensure that the only incoming field from infinity is

$$\eta^I = A^I \exp\left[ik(x\cos\theta^I + y\sin\theta^I)\right], \tag{9}$$

in which A^I and θ^I are the given amplitude and the given angle of incidence, respectively, for the incident field. In (8) $r = (x^2+y^2)^{\frac{1}{2}}$ and the scattered field η^S is defined through

$$\eta = \eta^I + \eta^S. \tag{10}$$

2.1. *Propagation*

We represent the spatial part of the surface elevation in the following asymptotic representation assuming k large:

$$\eta(x,y) = A\exp(ikS). \tag{11}$$

Here the amplitude $A = A(x,y)$ and the phase $S = S(x,y)$ are slowly varying functions of the position so that the rapid variation in the surface elevation is described through the phase factor $\exp(ikS)$. Insertion of (11) in the Helmholtz equation with the constant k replaced by the constant $k_1 = k + i\alpha$ yields

$$\{k^2(1-(\nabla S)^2)A + ik(2\nabla S\,.\,\nabla A + (2\alpha + \nabla^2 S)A) + \nabla^2 A - \alpha^2 A\}\exp(ikS) = 0. \tag{12}$$

By equating the coefficients k^2 and k to zero we obtain the eikonal equation

$$(\nabla S)^2 = 1, \tag{13}$$

and the transport equation

$$\nabla S\,.\,\nabla A + (\alpha + \tfrac{1}{2}\nabla^2 S)A = 0. \tag{14}$$

The eikonal equation may be integrated to give $S = s$, where s is the distance measured along the ray, which is straight (Larsen 1977*a*), thus yielding the phase factor $\exp(iks)$.

The transport equation may now be written

$$dA/ds + (\alpha + \tfrac{1}{2}\nabla^2 s)A = 0. \tag{15}$$

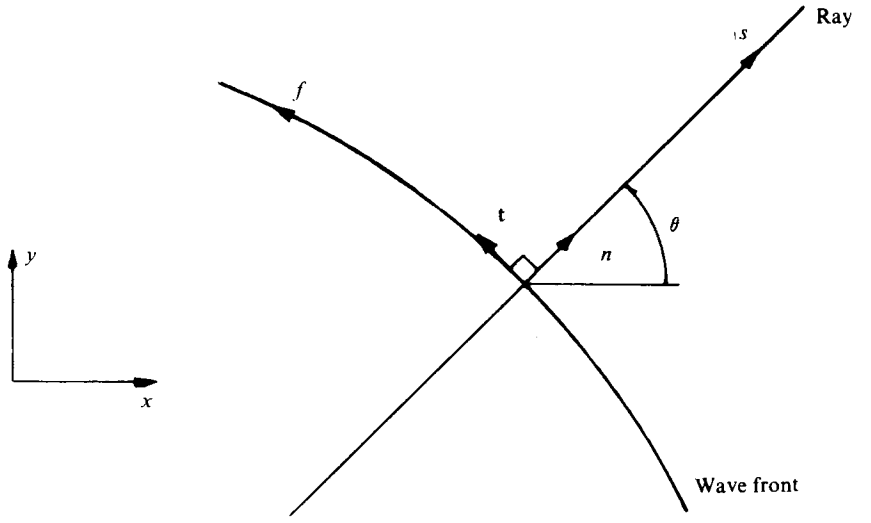

FIGURE 2. Wave front and ray.

The curves S = constant are the wave fronts and the orthogonals are the rays (figure 2). Let **n** and **t** be unit vectors along the ray and along the wave front respectively and f the arc length along the wave front; then

$$\nabla^2 s = \nabla . \mathbf{n} = \frac{d\mathbf{n}}{df} . \nabla f = \frac{d\theta}{df} = \kappa, \tag{16}$$

in which θ is the angle between the ray and the x axis (figure 2) and κ is the curvature of the wave front. Since the rays are straight the wave fronts are parallel, i.e. $\kappa = 0$ or $\kappa = 1/s$, where s now denotes the distance to a singular point of the ray system, e.g. a caustic point, a focal point, a source point, or an edge diffraction point (figure 3).

Integration of (15) with (16) inserted yields in the two cases

$$A = \text{constant} \times \exp(-\alpha s), \tag{17a}$$

or

$$A = \text{constant} \times \exp(-\alpha s)/s^{\frac{1}{2}}. \tag{17b}$$

If we apply the principle of energy conservation to a divergent pencil of rays we end up with the factor $s^{-\frac{1}{2}}$, which accordingly is called the divergence factor. The value of the constant in (17) must be determined from the amplitude of the incident field A^I or from a canonical problem.

In conclusion to the preceding remarks we note that, when the amplitude and phase at one point of a ray are known, the amplitude and phase at any other point of that ray can be calculated. This is the constructive aspect of the ray method.

For the field in the vicinity of singular points ($ks < 1$) uniform asymptotic methods must be applied (see, for example, Chao 1971); but we consider only the far field.

2.2. *Reflexion*

The canonical problem for the reflexion process is reflexion at a straight boundary. Waves incident from a direction forming an angle θ^I with the boundary and with amplitude A^I will excite reflected waves in the direction forming an angle θ^R with

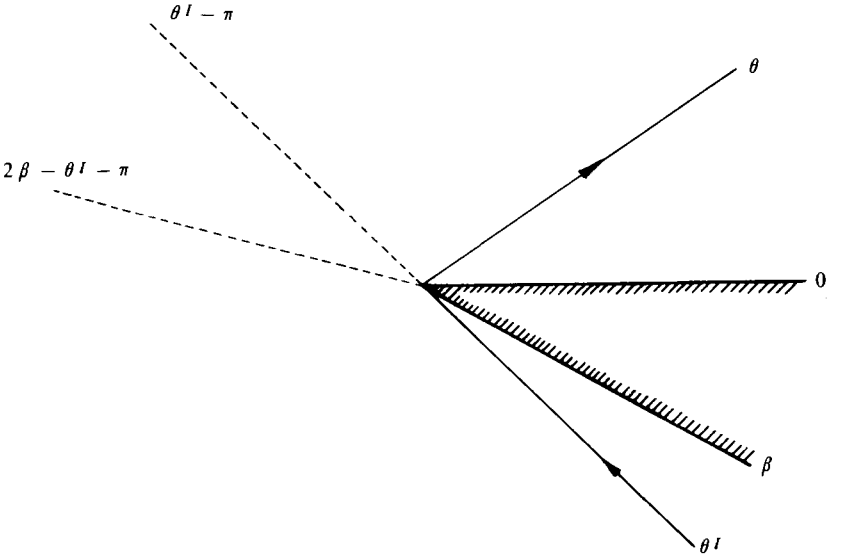

FIGURE 3. Diffraction at an edge point of the harbour boundary.

the boundary and with the amplitude RA^I, where R is the reflexion coefficient. Insertion of the total field $\eta = \eta^I + \eta^R$ in the surface impedance boundary condition (7) yields the law of reflexion

$$\theta^R = \theta^I, \tag{18}$$

and the reflexion coefficient $R = (\sin\theta^I - Z)/(\sin\theta^I + Z)$. (19)

In Larsen & Christiansen (1975) a real constant reflexion coefficient was used. An absorbing boundary will have $|R| \leqslant 1$ or $\mathrm{Re}\,(Z) \geqslant 0$. The surface impedance is determined by matching the reflexion coefficient given by (19) for normal incidence ($\theta^I = 90°$) with experimental and numerical results (see Miche 1951; Goda & Abe 1968; Madsen 1974; Madsen & White 1976). In contrast with Mei & Chen (1975) we use (19) with constant surface impedance in order to retain a linear boundary condition. Total reflexion ($R = 1$) corresponds to $Z = 0$.

2.3. *Edge diffraction*

A canonical problem for edge diffraction is a wedge as sketched in figure 3. We use the impedance boundary condition

$$\frac{1}{r}\frac{\partial\eta}{\partial\theta} + ikZ_+\eta = 0, \quad \theta = 0, \tag{20a}$$

and

$$\frac{1}{r}\frac{\partial\eta}{\partial\theta} - ikZ_-\eta = 0, \quad \theta = \beta. \tag{20b}$$

Here (r, θ) are polar co-ordinates (figure 3) and β is the outer opening angle of the wedge. The solution to the Helmholtz equation for plane wave incidence is composed of the incident field in the illuminated zone, the reflected field in the zone illuminated by the reflected field, and an edge-diffracted field. The solution was found by

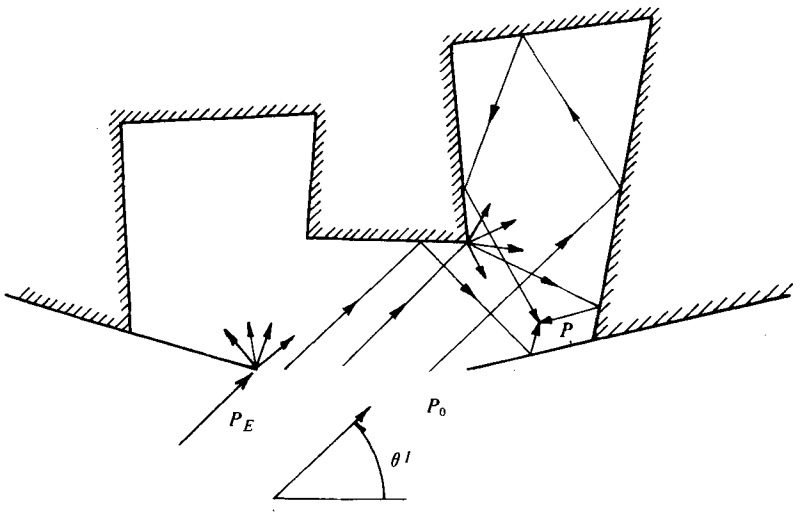

FIGURE 4. Typical harbour with ray system.

Malyughinetz (1960) [see also Hurd (1976) for the half-plane case]. We have used an approximate solution to the above-stated problem. For the edge-diffracted field η^D we use (see Larsen 1977*a*)

$$\eta^D = \eta^I \frac{\exp(iks)\exp(-\alpha s)}{s^{\frac{1}{2}}}\left[-\frac{\exp(\frac{1}{4}i\pi)}{(2\pi k)^{\frac{1}{2}}}\frac{\pi}{2\beta}\right]$$
$$\times\left[\cot\frac{\pi}{2\beta}(\pi+(\theta-\theta^I))+\cot\frac{\pi}{2\beta}(\pi-(\theta-\theta^I))\right.$$
$$\left.+\frac{|\sin(\beta-\theta^I)|-Z_-}{|\sin(\beta-\theta^I)|+Z_-}\cot\frac{\pi}{2\beta}(\pi+(\theta+\theta^I))+\frac{|\sin\theta^I|-Z_+}{|\sin\theta^I|+Z_+}\cot\frac{\pi}{2\beta}(\pi-(\theta+\theta^I))\right]. \quad (21)$$

In (21) we recognize the phase factor $\exp(iks)$, the divergence factor $s^{-\frac{1}{2}}$, and the attenuation factor due to bottom friction $\exp(-\alpha s)$. The remaining factor in (21) is called the diffraction coefficient and denoted $D_\beta(\theta,\theta^I;Z_\pm)$. The expression (21) is singular along shadow boundaries $\theta=\theta^I\pm\pi$ and along reflexion boundaries

$$\theta=\pi-\theta^I \quad \text{and} \quad \theta=2\beta-\pi-\theta^I.$$

This singular behaviour can be removed following Kouyoumjian & Pathak (1974) by multiplication of each term in (21) by a transition function cancelling the singularities in such a way that the diffracted field will possess discontinuities which make the total field continuous (see Larsen 1977*a*).

3. The computational method

We assume the harbour boundary to be composed of straight walls. A typical harbour geometry with waves incident from infinity is shown in figure 4. Multiply reflected rays are excited in accordance with the law of reflexion. In the figure two multiply reflected rays reaching the point P are shown. Diffracted rays occur when a ray strikes an edge point of the harbour boundary. In figure 4 three diffraction processes

of this type are shown. In general the field on the diffracted rays becomes weak and as a consequence we have only included singly diffracted rays in our calculations.

In accordance with the reciprocity principle the propagation direction along the ray can be inverted. This fact is exploited in the ray-tracing algorithm, which works as follows. A source is placed at the field point P radiating rays in all directions. The algorithm then singles out the rays that, possibly after multiple reflexions or single diffractions, can be identified with an inverted incident ray coming through the harbour entrance. In this way the radiation condition is fulfilled. For an account of the ray-tracing algorithm see Larsen (1977*b*).

The resultant field at the point P in the harbour produced by a multiply reflected ray becomes

$$\eta^R(P) = \eta^I(P_0) \exp[(ik-\alpha)s] \prod_n R_n, \tag{22}$$

where $\eta^I(P_0)$ is the incident field at point P_0 (figure 4), s is the distance from P_0 to P measured along the multiply reflected ray, and $\prod_n R_n$ is the product of the reflexion coefficients for the reflexion processes involved. No divergence factor is present in (22) since all members of each family of rays are parallel. The diffracted field at P due to a single diffraction process at an edge point P_E becomes

$$\eta^D(P) = [\sum_m \eta_m^G(P_E) D_{\beta_m}(\theta_m^I, \theta; Z_\pm)] \exp[(ik-\alpha)s^D] \prod_n R_n \frac{1}{(s^D)^{\frac{1}{2}}}. \tag{23}$$

In this expression the first factor contains a summation over the contributions $\eta_m^G(P_E)$ from each incident geometrical optics ray (characterized by the angle of incidence θ_m^I). The diffracted rays leave P_E under the angle θ and the diffraction process at P_E is described by the diffraction coefficient, $D_{\beta_m}(\theta_m^I, \theta; Z_\pm)$. The diffracted rays undergo a number of reflexions ($\prod_n R_n$) before reaching the point P. The distance measured along the diffracted ray from P_E to P is denoted s^D, and the divergence factor for this ray becomes $(s^D)^{-\frac{1}{2}}$.

The resultant field at P is

$$\eta(P) = \eta^I(P) + \Sigma\eta^R(P) + \Sigma\eta^D(P), \tag{24}$$

where we sum the contributions from all possible rays through P. However, the summation is truncated when the contributions become small owing to the various losses described previously. If P lies in the shadow region of the incident wave with respect to any edge point the first term in (24) vanishes.

4. Results and discussion

4.1. *The rectangular harbour*

For long wave excited resonance in a fully open rectangular harbour many analytical and experimental results are available, see Miles & Munk (1961), Ippen & Goda (1963), Hwang & Tuck (1970), Lee (1971), Ünlüata & Mei (1973) and Mei & Chen (1975). For shorter waves, however, the methods used in the references listed above fail or become impractical. In figure 5 we have shown the amplification factor $|\eta|/2A^I$ at the back wall of a fully open rectangular harbour versus the relative wavenumber kl, where l is the length of the harbour, a is the width of the harbour, and $a/l = 0{\cdot}194$.

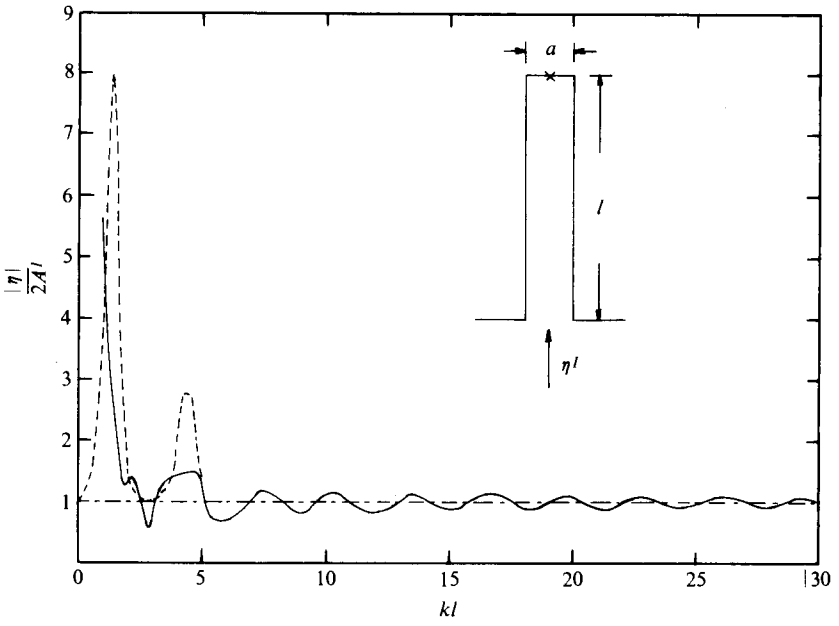

FIGURE 5. Amplification factor $|\eta|/2A^I$ versus relative wavenumber kl at the back wall of a fully open rectangular harbour: ——, ray method; – – –, finite element method (Mei & Chen 1975); — — —, geometrical optics field.

In the figure we have also plotted the results obtained by Mei & Chen (1975) using finite element methods in the range $0 < kl < 5$. These results show excellent agreement with experimental data. For small values of kl we cannot expect the ray method to be valid; but we do find some agreement with respect to the position of the relative maxima and minima of the two response curves. Mei & Chen (1975) do not show results for kl larger than 5, a fact which might be explained by the difficulties in exploiting finite element or finite difference methods for high-frequency waves.

In order to compare our results with some obtained by a finite difference method (Danish Hydraulic Institute, private communication) we have computed the relative amplitude in the harbour shown in figure 6. The finite difference method is based on nonlinear Boussinesq equations which are only approximately satisfied by sinusoidal solutions. Moreover no special treatment of the corners is used. The waves are sinusoidal and normally incident on the northern boundary. The southern boundary is fully absorbing ($R = 0$) and the remaining boundary and the breakwater are fully reflecting ($R = 1$). The diffraction effects of the corners at the northern and southern boundaries are suppressed in order that the comparison can be carried out. In table 1 we have listed the relative amplitudes obtained using the two methods. The wavelength is $L = 93{\cdot}4$ m. The agreement between the results is excellent taking into consideration the differences between the two methods.

4.2. *Hanstholm Harbour*

In order to show the capability of the ray method we have applied it to a harbour of a more complicated shape. A sketch of the planform, which is an approximation of the outer basin of Hanstholm Harbour, Denmark, is shown in figure 7. The entrance

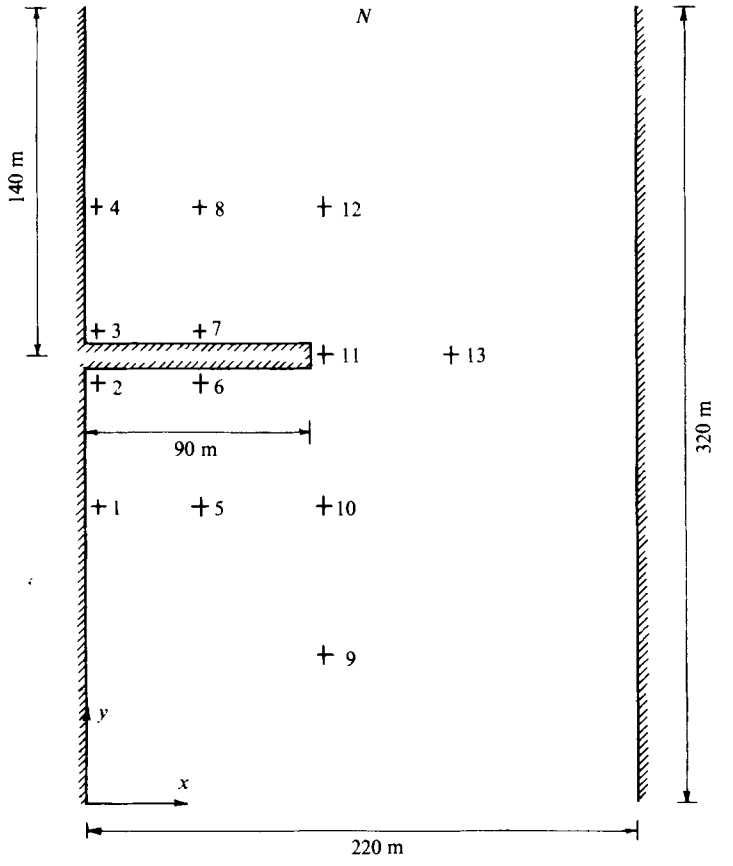

FIGURE 6. Rectangular harbour with breakwater.

Point	x/m	y/m	Finite difference method $\lvert\eta\rvert/A^I$	Ray method $\lvert\eta\rvert/A^I$
1	5	120	0·34	0·33
2	5	170	0·46	0·36
3	5	190	1·8	1·6
4	5	240	1·4	1·8
5	45	120	0·38	0·36
6	45	170	0·36	0·41
7	45	190	2·2	2·3
8	45	240	1·8	1·9
9	95	60	0·55	0·60
10	95	120	0·55	0·50
11	95	180	1·2	1·0
12	95	240	1·0	1·3
13	145	180	1·0	1·1

TABLE 1. Comparison between the relative amplitudes of the points marked in figure 6 using a finite difference method (Danish Hydraulic Institute, private communication) and the ray method.

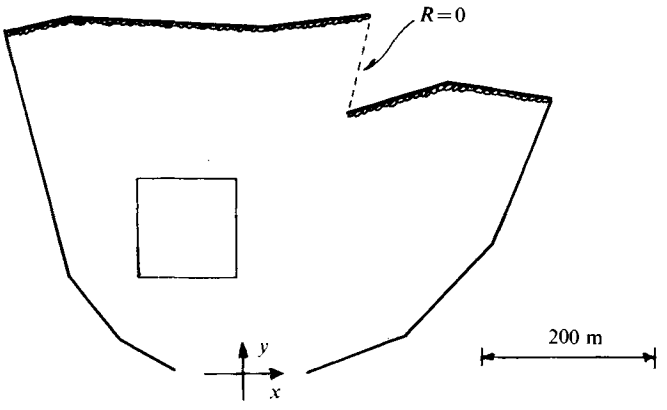

FIGURE 7. Outer basin of Hanstholm Harbour. The back walls are strongly dissipative.

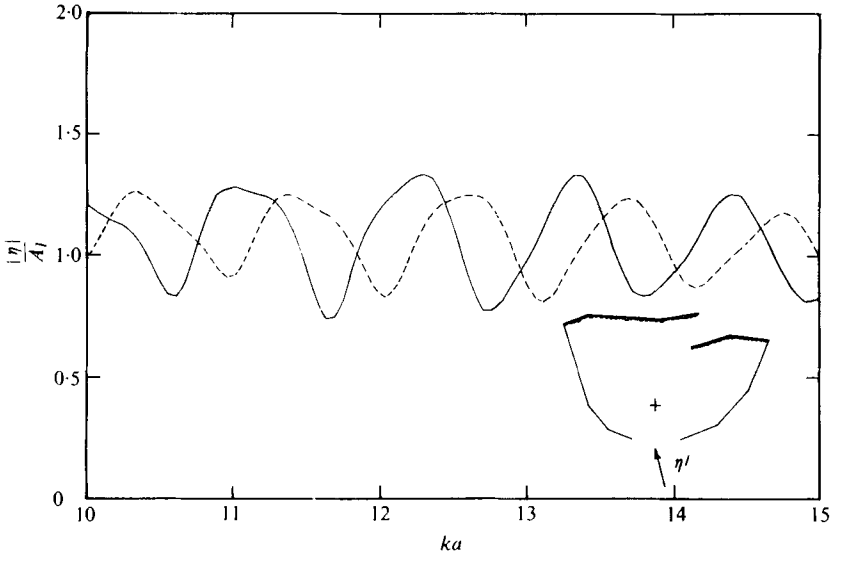

FIGURE 8. Relative amplitude $|\eta|/A^I$ versus relative wavenumber ka at the point $(x, y) = (0\,\text{m}, 100\,\text{m})$ in Hanstholm Harbour: ——, for real surface impedances (see text); – – –, for complex surface impedances (see text). $\theta^I = 102°$.

to the inner basins is considered fully absorbing ($R = 0$, see figure 7). The back walls are made of large concrete blocks and are accordingly strongly dissipative. Hence we use a small reflexion coefficient for the back walls, $R = 0{\cdot}33$ for normal incidence corresponding to $Z = 0{\cdot}5$. For the outer breakwaters we use $R = 0{\cdot}85$ for normal incidence corresponding to $Z = 0{\cdot}08$. In order to investigate a change in the reflexion coefficients we have also carried out the calculations for $Z = 0{\cdot}66 + 0{\cdot}25i$ for the back walls and $Z = 0{\cdot}09 + 0{\cdot}41i$ for the outer breakwaters. The water depth is taken to be constant and equal to $h = 6$ m and the friction parameter k_N is taken to be $k_N = 0{\cdot}20$ m.

In figure 8 we have shown the relative amplitude $|\eta|/A^I$ at the point $(x, y) = (0\,\text{m}, 100\,\text{m})$ versus the relative wavenumber ka, where $a = 146$ m is the width of the harbour entrance. The angle of incidence is $\theta^I = 102°$ (figure 7). We have shown the results for the two sets of surface impedances mentioned above. We have repeated

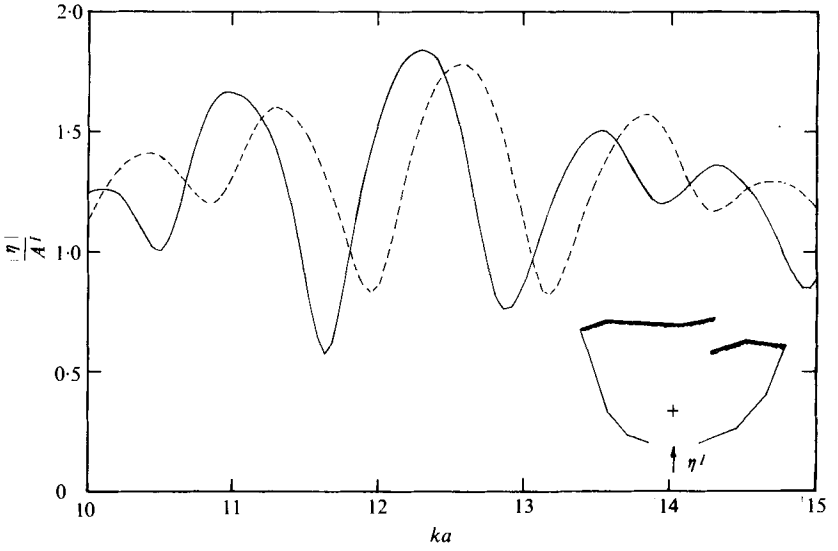

FIGURE 9. Relative amplitude $|\eta|/A^I$ versus relative wavenumber ka at the point $(x, y) =$ (0 m, 100 m) in Hanstholm Harbour: ——, for real surface impedances (see text); – – –, for complex surface impedances (see text). $\theta^I = 90°$.

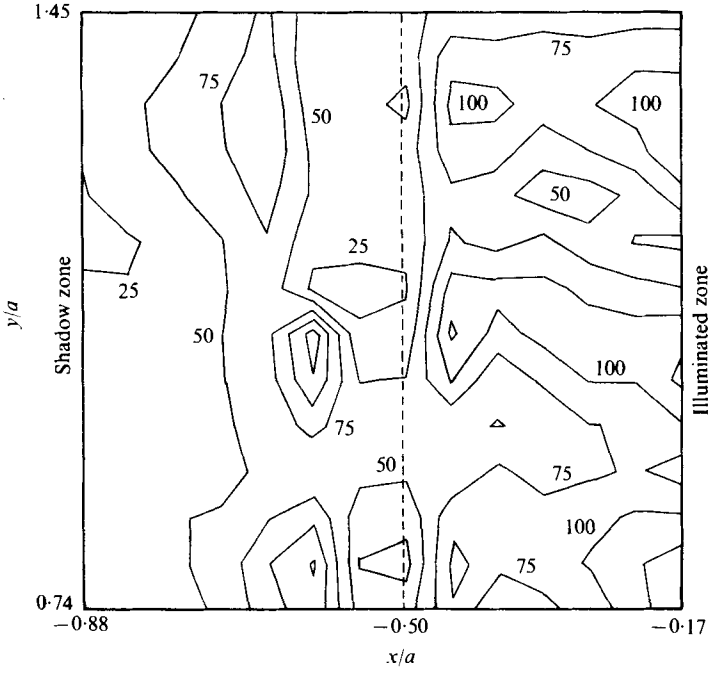

FIGURE 10. Contour map of the relative amplitude in the square area of figure 7 for real surface impedances (see text) and $ka = 11{\cdot}63$. $\theta^I = 90°$.

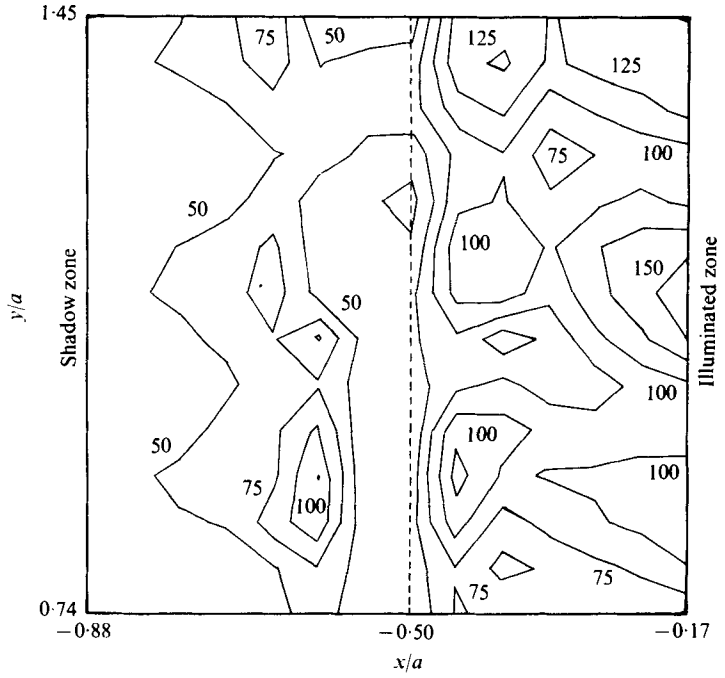

FIGURE 11. Contour map of the relative amplitude in the square area of figure 7 for real surface impedances (see text) and $ka = 12{\cdot}30$. $\theta^I = 90°$.

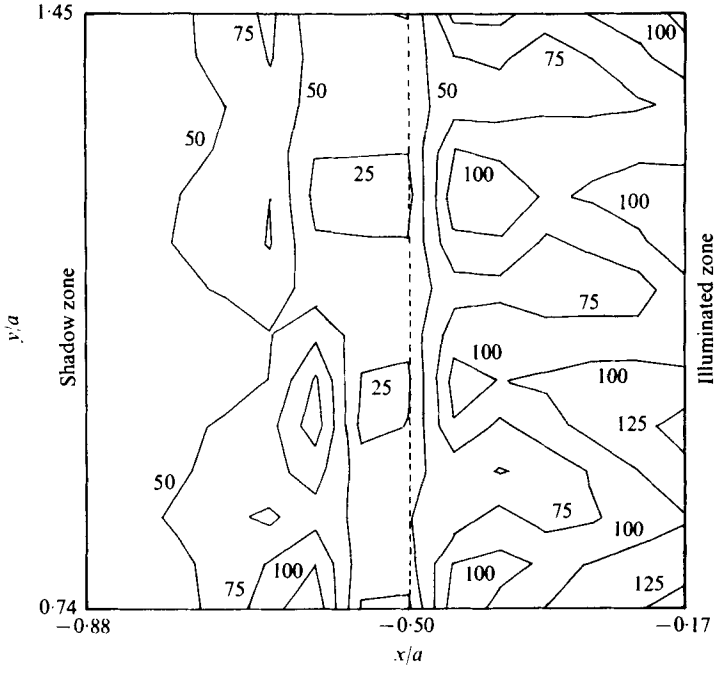

FIGURE 12. Contour map of the relative amplitude in the square area of figure 7 for complex surface impedances (see text) and $ka = 13{\cdot}16$. $\theta^I = 90°$.

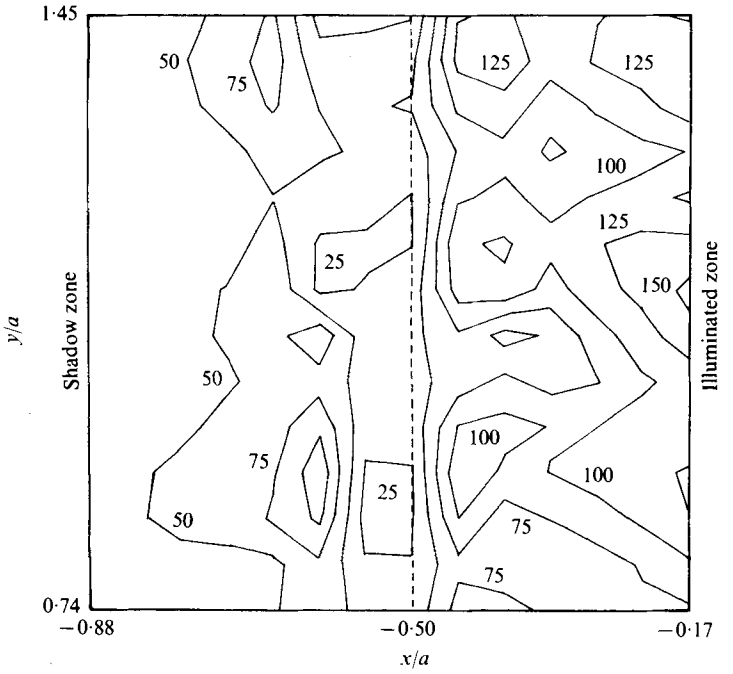

FIGURE 13. Contour map of the relative amplitude in the square area of figure 7 for complex surface impedances (see text) and $ka = 12{\cdot}55$. $\theta^I = 90°$.

the calculation for waves normally incident on the harbour entrance ($\theta^I = 90°$) as shown in figure 9. In both cases we observe that the change in the reflexion coefficient mainly results in a translation of the response curves. Since the field point is in the centre of the incident field for $\theta^I = 90°$, we observe the strongest amplification here. For waves incident normally on the harbour entrance we have made contour maps of the relative amplitude in the square area of figure 7. In figure 10 and figure 11 we have shown the results for the real surface impedances for $ka = 11{\cdot}63$ and $ka = 12{\cdot}30$ respectively. We observe a strong dependence of the amplitude on position.

In figure 12 and figure 13 we have repeated the calculations for the complex surface impedances mentioned above for $ka = 13{\cdot}16$ and $ka = 12{\cdot}55$ respectively. The change in the surface impedances does not affect the picture as much as the change in relative wavenumber. In all cases we observe a weaker field in the shadow zone for the incident field than in the illuminated zone (figure 7).

The author wishes to thank his thesis advisers, Professor Erik B. Hansen and Associate Professor Peter Leth Christiansen, for suggesting this problem and offering guidance and encouragement throughout the course of the study. Associate Professor Ivar G. Jonsson, The Institute of Hydrodynamics and Hydraulic Engineering (ISVA), is thanked for several informative discussions on the subject. This work was supported by the Danish Council for Scientific and Technical Research, DK-1060, Copenhagen, Denmark.

REFERENCES

BERKHOFF, J. C. W. 1973 Computation of combined refraction–diffraction. *Proc. 13th Coastal Engng Conf. July* 1972, *Vancouver*, vol. 1, pp. 471–490. New York: A.S.C.E.

BLUE, F. L. & JOHNSON, J. W. 1949 Diffraction of waves passing through a breakwater gap. *Trans. Am. Geophys. Un.* **30**, 705–718.

CARR, J. H. 1952 Wave protection aspects of harbor design. *Hydrodynamics Lab., Cal. Inst. Tech. Rep.* E-11.

CHAO, Y.-Y. 1971 An asymptotic evaluation of the wave field near a smooth caustic. *J. Geophys. Res.* **76**, 7401–7408.

CHRISTIANSEN, P. L. 1975 Diffraction of gravity waves by large islands. *Proc. 14th Coastal Engng Conf. July* 1974, *Copenhagen*, vol. 1, pp. 601–614. New York: A.S.C.E.

CHRISTIANSEN, P. L. 1976 Diffraction of gravity waves by ray methods. *Proc. Int. Symp. Waves on Varying Depth, July* 1976, *Canberra*. (To be published.)

GODA, Y. & ABE, Y. 1968 Apparent coefficient of partial reflection of finite amplitude waves. *Rep. Port and Harbour Res. Inst.* no. 7, pp. 3–53.

HURD, R. A. 1976 The Wiener–Hopf–Hilbert method for diffraction problems. *Can. J. Phys.* **54**, 775–780.

HWANG, L.-S. & TUCK, E. O. 1970 On the oscillations of harbors of arbitrary shape. *J. Fluid Mech.* **42**, 447–464.

IPPEN, A. T. (ed.) 1966 *Estuary and Coastal Hydrodynamics*. McGraw-Hill.

IPPEN, A. T. & GODA, Y. 1963 Wave induced oscillations in harbors: the solution for a rectangular harbour connected to the open sea. *Hydrodynamics Lab., M.I.T. Rep.* no. 59.

JONSSON, I. G. 1975 The wave friction factor revisited. *Inst. Hydrodyn. Hydraulic Engng (I.S.V.A.), Tech. Univ. Denmark, Prog. Rep.* no. 37, pp. 3–8.

KELLER, J. B. 1958 Surface waves on water of non-uniform depth. *J. Fluid Mech.* **4**, 607–614.

KELLER, J. B. 1962 Geometrical theory of diffraction. *J. Optical Soc. Am.* **52**, 116–130.

KOUYOUMJIAN, R. G. & PATHAK, P. H. 1974 A uniform geometrical theory of diffraction for an edge in a perfectly conducting surface. *Proc. I.E.E.E.* **62**, 1448–1461.

LARSEN, J. 1977*a* Computation of harbour oscillations by ray methods. Ph.D. thesis, Tech. Univ. Denmark (*DCAMM Rep.* S8).

LARSEN, J. 1977*b* A ray-tracing algorithm. To appear.

LARSEN, J. & CHRISTIANSEN, P. L. 1975 Computations of harbor oscillations by ray methods. *Proc. Symp. Modeling Techniques, Sept.* 1975, *SanFrancisco*, vol. 2, pp. 888–906. New York: A.S.C.E.

LEE, J.-J. 1971 Wave-induced oscillations in harbours of arbitrary geometry. *J. Fluid Mech.* **45**, 375–394.

MADSEN, O. S. 1974 Wave transmission through porous structures. *Proc. A.S.C.E., J. Waterways, Harbors & Coastal Engng Div.* **100**, 169–188.

MADSEN, O. S. & WHITE, S. M. 1976 Energy dissipation on a rough slope. *Proc. A.S.C.E., J. Waterways, Harbors & Coastal Engng Div.* **102**, 31–48.

MALYUGHINETZ, G. D. 1960 Das Sommerfeldsche Integral und die Lösung von Beugungsaufgaben in Winkelgebieten. *Ann. Phys.* **1**, 107–122.

MEI, C. C. & CHEN, H. S. 1975 Hybrid-element method for water waves. *Proc. Symp. Modeling Techniques, Sept.* 1975, *San Francisco*, vol. 1, pp. 63–81, New York: A.S.C.E.

MICHE, M. 1951 Le pouvoir réfléchissant des ouvrages maritimes exposés à l'action de la houle. *Annales des Ponts et Chaussées* **121**, 285–319.

MILES, J. W. & MUNK, W. 1961 Harbor paradox. *Proc. A.S.C.E., J. Waterways, Harbors and Coastal Engng Div.* **87**, 111–131.

PENNEY, W. G. & PRICE, A. T. 1944 Diffraction of water waves by breakwaters. *Directorate of Miscellaneous Weapons Development, Technical History* 26, *Artificial Harbors*, §§ 3–4.

SHEN, M. C. 1975 Ray method for surface waves on fluid of variable depth. *SIAM Rev.* **17**. 38–56.

SHEN, M. C., MEYER, R. E. & KELLER, J. B. 1968 Spectra of water waves in channels and around islands. *Phys. Fluids* **11**, 2289–2304.

SMITH, R. & SPRINKS, T. 1975 Scattering of surface waves by a conical island. *J. Fluid Mech.* **72**, 373–384.

SOMMERFELD, A. 1896 Mathematische Theorie der Diffraktion. *Math. Ann.* **47**, 317–374.

ÜNLÜATA, Ü. & MEI, C. C. 1973 Long wave excitation in harbours – an analytical study. *Ralph M. Parsons Lab. Water Resources Hydrodynamics, M.I.T. Rep.* no. 171.